

Dynamical Supersymmetry Breaking from Meta-stable Vacua in an $\mathcal{N} = 1$ Supersymmetric Gauge Theory

Masato Arai ^{a*}, Claus Montonen ^{a†}, Nobuchika Okada ^{b‡}
and
Shin Sasaki ^{a§}

^a *High Energy Physics Division, Department of Physical Sciences, University of Helsinki
and Helsinki Institute of Physics, P.O.Box 64, FIN-00014, Finland*

^b *Theory Division, KEK, Tsukuba 305-0801, Japan*

Abstract

We investigate supersymmetry breaking meta-stable vacua in $\mathcal{N} = 2$, $SU(2) \times U(1)$ gauge theory with $N_f = 2$ massless flavors perturbed by the addition of small $\mathcal{N} = 1$ preserving mass terms in a presence of a Fayet-Iliopoulos term. We derive the low energy effective theory by using the exact results of $\mathcal{N} = 2$ supersymmetric QCD and examine the effective potential. At the classical level, the theory has supersymmetric vacua on Coulomb and Higgs branches. We find that supersymmetry on the Coulomb branch is dynamically broken as a consequence of the strong dynamics of $SU(2)$ gauge symmetry while the supersymmetric vacuum on the Higgs branch remains. We also estimate the lifetimes of the local minima on the Coulomb branch. We find that they are sufficiently long and therefore the local vacua we find are meta-stable.

^{*}masato.arai@helsinki.fi

[†]claus.montonen@helsinki.fi

[‡]nobuchika.okada@kek.jp

[§]shin.sasaki@helsinki.fi

Contents

1	Introduction	2
2	The model	4
3	Quantum theory	6
3.1	Effective action and monodromy	6
3.2	Effective potential	8
4	Numerical analysis	10
4.1	Singular points	10
4.2	Numerical calculation	11
5	Decay rate of the local vacuum	17
6	Conclusion and discussion	20
A	Explicit form of the effective couplings	20

1 Introduction

Supersymmetry (SUSY) is the most promising and best motivated framework for extending the Standard Model. However, nature turns out to be not supersymmetric at the electroweak scale and therefore SUSY must be broken. The origin of the SUSY breaking is still a prime open question. It is reasonable that SUSY is broken dynamically. Indeed, dynamical SUSY breaking provides a natural explanation for the gauge hierarchy problem [1]. The important fact in dynamical SUSY breaking is that if SUSY is not broken at tree level, it remains unbroken to all orders of perturbative corrections because of the non-renormalization theorem [2]. This implies that SUSY is dynamically broken only by non-perturbative effects such as instanton corrections. Thus, understanding of gauge dynamics is crucial to study dynamical SUSY breaking.

There has been much progress in understanding the gauge dynamics of strongly coupled $\mathcal{N} = 1$ SUSY field theory with N_c color and $N_f \leq N_c + 1$ flavors [3, 4]. The exact low energy effective superpotential can be derived by using the holomorphy properties of the superpotential and the gauge kinetic function. This progress has triggered the discovery of many new SUSY breaking theories, as well as new techniques for establishing SUSY breaking. One of the interesting models with dynamical SUSY breaking is the Izawa-Yanagida-Intriligator-Thomas model [5, 6]. In this model, an O’Raifeartaigh type sector is dynamically generated in the low energy superpotential. Therefore, SUSY is spontaneously broken. However, this SUSY breaking vacuum is degenerate *i.e.* there exists a pseudo flat direction. In order to remove this degeneracy, we have to take

account of quantum corrections for the Kähler potential. In general, this is a very difficult task since the Kähler potential is not holomorphic and thus quantum corrections can be estimated at best by perturbative means. Such an estimation is possible only in the ultraviolet (weak coupling) region of the moduli space parameterizing the pseudo flat direction which is far from the origin. Therefore, the potential behavior in the infrared region remains unclear.

This situation is changed for $\mathcal{N} = 1$ SUSY QCD with N_c colors and $N_c + 1 \leq N_f < \frac{3}{2}N_c$ flavors [7]. In this flavor region, the O’Raifeartaigh type model arises as the low energy effective theory of the magnetic dual and the effective theory is infrared free. This is contrary to the Izawa-Yanagida-Intriligator-Thomas model where the gauge coupling strength becomes strong at low energies. This property makes it possible to calculate perturbative corrections to the Kähler potential in the infrared region. Indeed, in [7] it is found that one-loop corrections to the Kähler potential remove the degeneracy of the pseudo flat direction and that there is a stabilized SUSY breaking vacuum at the origin of the moduli space. In addition to this vacuum, there are also N_c dynamically generated SUSY vacua at points far from the origin which are expected to exist by the argument of the Witten index. Thus the SUSY breaking vacuum at the origin is a local vacuum. Furthermore, the local vacuum can be long-lived compared to the age of the universe by choosing appropriate values of parameters in the theory. Therefore this local vacuum is meta-stable.

As was mentioned above, in $\mathcal{N} = 1$ SUSY models, one can estimate quantum corrections to the Kähler potential only in a weak coupling region by perturbative means. However, in an $\mathcal{N} = 2$ SUSY gauge theory one can derive the exact low energy effective action as was demonstrated by Seiberg and Witten [8, 9], using the properties of holomorphy and duality. In [10], we studied meta-stable vacua in an $\mathcal{N} = 2$ $SU(2) \times U(1)$ SUSY gauge theory with $N_f = 2$ massless flavors including a Fayet-Iliopoulos (FI) D -term, by using the original analysis in [11]. Due to the FI term, the theory exhibits tree-level SUSY breaking on the Coulomb branch in almost all of the moduli space except near the origin. Around the origin along the Coulomb branch, there is an unstable direction to the Higgs branch where a SUSY vacuum exists. In this model, we demonstrated that there is a long-lived local minimum on the Coulomb branch in which the SUSY and $U(1)_R$ symmetry is dynamically broken in the non-perturbative region. We showed that the decay rates from the local minimum to the runaway SUSY vacuum and also to the SUSY vacua on the Higgs branch are actually very small. Moreover, we pointed out that massive hypermultiplets in the model can play the role of messenger fields in the gauge mediation scenario if a part of the flavor symmetry among the hypermultiplets is gauged and identified with the Standard Model gauge group.

It is also possible to derive the exact low energy effective action in the $\mathcal{N} = 1$ theory based on the $\mathcal{N} = 2$ theory perturbed by terms preserving $\mathcal{N} = 1$ SUSY. Assuming that the perturbation does not affect the gauge dynamics in the original $\mathcal{N} = 2$ theory, we can use the result of the Seiberg-Witten theory. In [12, 13, 14], it was shown that there can be a meta-stable SUSY breaking vacuum in the Seiberg-Witten theory with terms preserving $\mathcal{N} = 1$ SUSY. M-theory brane configurations corresponding to these perturbed Seiberg-Witten theories were discussed in [15, 16].

In this paper, we investigate a model based on $\mathcal{N} = 2$ SUSY gauge theory realizing dynamical SUSY breaking in meta-stable vacua. The model we consider is an $\mathcal{N} = 2$, $SU(2) \times U(1)$ gauge

theory with $N_f = 2$ massless hypermultiplets perturbed by $\mathcal{N} = 1$ preserving adjoint mass terms and a linear term (the FI F -term). Although, in this model, only $\mathcal{N} = 1$ SUSY is preserved by the perturbation to the superpotential, the quantum theory can be analyzed by extending the Seiberg-Witten solution, provided that the mass parameters μ_i and linear term parameter λ are very small compared to the $SU(2)$ dynamical scale Λ . In the classical theory of our model, there are SUSY vacua on the Coulomb branch and the Higgs branch. We will show that the SUSY vacua on the Coulomb branch are dynamically broken as a consequence of the strong dynamics of the $SU(2)$ gauge coupling while the SUSY vacuum on the Higgs branch remains. We will also show that the decay rate from the local vacua to the SUSY vacuum can be very small with an appropriate choice of parameters. Therefore, we will find meta-stable SUSY breaking vacua.

The organization of this paper is as follows. In section 2, we introduce our model and analyze the classical vacua. In section 3, the low-energy effective action is derived by using exact results of $\mathcal{N} = 2$ SUSY QCD. In section 4, the numerical analysis of the effective potential is presented. Section 5 is devoted to the decay rate estimation of the meta-stable SUSY vacua found in section 4. Section 6 is our conclusion. In Appendix A, the formulas necessary for the potential analysis are given.

2 The model

Let us first consider a tree-level Lagrangian of an $\mathcal{N} = 2$, $SU(2) \times U(1)$ gauge theory with $N_f = 2$ massless fundamental flavors Q and \tilde{Q}

$$\begin{aligned} \mathcal{L}^{\mathcal{N}=2} = & \frac{1}{2\pi} \text{Im} \left[\text{Tr} \left\{ \tau_{22} \left(\int d^4\theta A_2^\dagger e^{2V_2} A_2 e^{-2V_2} + \frac{1}{2} \int d^2\theta W_2^2 \right) \right\} \right] \\ & + \frac{1}{4\pi} \text{Im} \left[\tau_{11} \left(\int d^4\theta A_1^\dagger A_1 + \frac{1}{2} \int d^2\theta W_1^2 \right) \right] \\ & + \int d^4\theta \left[Q_r^\dagger e^{2V_2+2V_1} Q^r + \tilde{Q}_r e^{-2V_2-2V_1} \tilde{Q}^{r\dagger} \right] + \sqrt{2} \left[\int d^2\theta \tilde{Q}_r (A_2 + A_1) Q^r + h.c. \right]. \end{aligned} \quad (2.1)$$

Here, V_2, A_2 and V_1, A_1 correspond to $SU(2)$ and $U(1)$ vector multiplets respectively. The chiral superfields Q_I^r and \tilde{Q}_r^I are hypermultiplets that are in the fundamental and anti-fundamental representations of the $SU(2)$ gauge group ($r = 1, 2$ is the flavor index, and $I = 1, 2$ is the $SU(2)$ color index). The superfield strength is defined by $W_{i\alpha} = -\frac{1}{4} \bar{D}^2 (e^{-2V_i} D_\alpha e^{2V_i})$ ($i = 1, 2$). The complex gauge couplings are defined by

$$\tau_{22} = i \frac{4\pi}{g^2} + \frac{\theta}{2\pi}, \quad \tau_{11} = i \frac{4\pi}{e^2}, \quad (2.2)$$

where τ_{22} corresponds to an $SU(2)$ complex gauge coupling and τ_{11} is a $U(1)$ gauge coupling. The common $U(1)$ charge for the hypermultiplet is normalized to be 1. The $SU(2)$ generators T^a are normalized as $\text{Tr}(T^a T^b) = \frac{1}{2} \delta^{ab}$. The global symmetry in this theory is $SU(2)_{\text{left}} \times SU(2)_{\text{right}} \times SU(2)_R \times U(1)_R$.

Let us introduce mass and linear terms for the chiral superfields A_1, A_2 ,

$$\mathcal{L}_{\text{soft}} = \int d^2\theta \left(\mu_2 \text{Tr}(A_2^2) + \frac{1}{2} \mu_1 A_1^2 + \lambda A_1 \right) + h.c. \quad (2.3)$$

These terms break $\mathcal{N} = 2$ SUSY down to $\mathcal{N} = 1$. The dimensionful parameters μ_i can be taken to be real and positive without loss of generality, while we fix the dimensionless parameter λ to be real and positive, $\lambda > 0$, for simplicity. The linear term in A_1 is the FI term. In general, the FI term also appears in the D -term, but the $SU(2)_R$ symmetry allows us to take a frame so that it appears only in the F -term. Therefore, the $SU(2)_R$ symmetry is explicitly broken down to its subgroup $U'(1)_R$. The superpotential (2.3) also breaks $U(1)_R$ symmetry. The global symmetry of the theory turns out to be $SU(2)_{\text{left}} \times SU(2)_{\text{right}} \times U'(1)_R$. The scalar potential is easily derived from the Lagrangian $\mathcal{L} = \mathcal{L}^{\mathcal{N}=2} + \mathcal{L}_{\text{soft}}$

$$\begin{aligned} V(a_1, a_2, q, \tilde{q}) = & g^2 \text{Tr}[A_2, A_2^\dagger]^2 + \frac{g^2}{2} (q_r^\dagger T^a q^r - \tilde{q}_r T^a \tilde{q}^{\dagger r})^2 \\ & + q_r^\dagger [A_2, A_2^\dagger] q^r - \tilde{q}_r [A_2, A_2^\dagger] \tilde{q}^{\dagger r} + 2g^2 |\tilde{q}_r T^a q^r|^2 + \frac{e^2}{2} (q_r^\dagger q^r - \tilde{q}_r \tilde{q}^{\dagger r})^2 \\ & + 2 (q_r^\dagger |A_2 + A_1|^2 q^r + \tilde{q}_r |A_2 + A_1|^2 \tilde{q}^{\dagger r}) + \sqrt{2} \mu_2 g^2 (\tilde{q}_r T^a q^r A_2^a + h.c.) \\ & + \mu_2^2 g^2 A_2^{a\dagger} A_2^a + e^2 |\lambda + \mu_1 A_1 + \sqrt{2} q_r \tilde{q}^r|^2 \end{aligned} \quad (2.4)$$

where A_1, A_2, q^r and \tilde{q}_r are scalar components in the corresponding chiral superfields. Without the mass and linear terms, there is a SUSY vacuum on the Coulomb branch,

$$A_2 = \begin{pmatrix} a_2 & 0 \\ 0 & -a_2 \end{pmatrix}, \quad A_1 = a_1, \quad (2.5)$$

where a_1 and a_2 are the moduli of the vacuum. In this vacuum, the gauge symmetry is broken to $U(1)_c \times U(1)$. When turning on the mass and the FI terms, only the following point in the moduli space is left as a SUSY vacuum

$$q_r = \tilde{q}_r = 0, \quad A_2 = 0, \quad A_1 = -\frac{\lambda}{\mu_1}, \quad (2.6)$$

where the $SU(2)$ gauge symmetry is recovered. In addition to this SUSY vacuum on the Coulomb branch, there is another SUSY vacuum on the Higgs branch given by

$$\begin{aligned} q_I^1 = \tilde{q}_I^{1T} = \begin{pmatrix} u \\ v \end{pmatrix}, \quad q_I^2 = \tilde{q}_I^{2T} = \begin{pmatrix} v \\ -u \end{pmatrix}, \quad u, v \in \mathbf{C}, \\ u^2 + v^2 = \frac{-\lambda}{2\sqrt{2}}, \quad A_2 = A_1 = 0. \end{aligned} \quad (2.7)$$

In the following, we focus on the Coulomb branch and proceed to investigate the low-energy effective action.

3 Quantum theory

3.1 Effective action and monodromy

The exact low energy Wilsonian effective Lagrangian can be derived by integrating the action to zero momentum. In our case, the resultant Lagrangian could be described by light fields, the dynamical scale, the masses $\mu_i (i = 1, 2)$ and the coefficient of the FI term λ . However, since it is in general very difficult to implement the integration, we assume that μ_i and λ are much smaller than the dynamical scale of the $SU(2)$ gauge interaction Λ , *i.e.* $\mu_i \ll \Lambda$ and $\lambda \ll \Lambda^2$. This setup allows us to expand the exact low energy Lagrangian $\mathcal{L}_{\text{exact}}$ with respect to the parameters μ_i and λ as

$$\mathcal{L}_{\text{exact}} = \mathcal{L}_{\text{SUSY}} + \mathcal{L}_{\text{soft}} + \mathcal{O}(\mu_i^2, \lambda). \quad (3.1)$$

Here the first term $\mathcal{L}_{\text{SUSY}}$ describes an $\mathcal{N} = 2$ SUSY Lagrangian containing full quantum corrections. The second term $\mathcal{L}_{\text{soft}}$ includes the masses and the FI terms in the leading order. In the following, we consider the effective action up to the leading order in μ_i and λ .

First we clarify the structure of the moduli space of the theory. As we have seen in the previous section, without the soft term (2.3), the theory has a moduli space parameterized by a_2 and a_1 on the Coulomb branch. Except at the origin of the moduli space the gauge symmetry is broken down to $U(1)_c \times U(1)$. Note that this $U(1)$ gauge interaction is treated as a cut-off theory [11, 10]. Thus, the Landau pole Λ_L is inevitably introduced in our effective theory, and the defining region of the modulus parameter a_1 is constrained to lie within the region $|a_1| < \Lambda_L$. Because of this constraint, the defining region for the modulus parameter a_2 is also constrained to be in the same region, since the two moduli parameters are related to each other through the hypermultiplets. We take the scale Λ_L to be much larger than the dynamical scale of the $SU(2)$ gauge interaction Λ as in [11, 10] (The explicit scale of Λ_L is given at the end of this section). This condition guarantees that the $U(1)$ gauge interaction is always weak in the defining region of moduli space. Note that in our framework we implicitly assume that the $U(1)$ gauge interaction has no effect on the $SU(2)$ gauge dynamics. This assumption will be justified in the following discussion concerning the monodromy transformation.

First we consider the general formulas for the effective Lagrangian $\mathcal{L}_{\text{SUSY}}$. The Lagrangian $\mathcal{L}_{\text{SUSY}}$ is given by two parts, vector multiplet part \mathcal{L}_{VM} and hypermultiplet part \mathcal{L}_{HM} ;

$$\mathcal{L}_{\text{SUSY}} = \mathcal{L}_{\text{VM}} + \mathcal{L}_{\text{HM}}. \quad (3.2)$$

The \mathcal{L}_{VM} part consists of $U(1)_c$ and $U(1)$ vector multiplets. The $U(1)_c$ vector multiplet (A_2, V_2) originates from the unbroken part (Cartan subalgebra) of the classical $SU(2)$ vector multiplet whereas (A_1, V_1) belongs to the $U(1)$ gauge multiplet which is left unbroken from the classical level. The effective Lagrangian for these vector multiplets is

$$\mathcal{L}_{\text{VM}} = \frac{1}{4\pi} \text{Im} \sum_{i,j=1}^2 \left[\int d^4\theta \frac{\partial \mathcal{F}}{\partial A_i} A_i^\dagger + \frac{1}{2} \int d^2\theta \tau_{ij} W_i W_j \right], \quad (3.3)$$

where $\mathcal{F} = \mathcal{F}(A_2, A_1, \Lambda, \Lambda_L)$ is a prepotential as will be discussed below. The effective gauge

coupling τ_{ij} is defined by

$$\tau_{ij} = \frac{\partial^2 \mathcal{F}}{\partial a_i \partial a_j}, \quad b_{ij} \equiv \frac{1}{4\pi} \text{Im}(\tau_{ij}) \quad (i, j = 1, 2). \quad (3.4)$$

The hypermultiplet part \mathcal{L}_{HM} is

$$\begin{aligned} \mathcal{L}_{\text{HM}} = & \int d^4\theta \left[M_r^\dagger e^{2n_m V_{2D} + 2n_e V_2 + 2n V_1} M^r + \tilde{M}_r e^{-2n_m V_{2D} - 2n_e V_2 - 2n V_1} \tilde{M}^{r\dagger} \right] \\ & + \sqrt{2} \int d^2\theta \left[\tilde{M}_r (n_m A_{2D} + n_e A_2 + n A_1) M^r + h.c. \right], \end{aligned} \quad (3.5)$$

where M^r, \tilde{M}_r are chiral superfields and V_{2D}, A_{2D} are dual variables of V_2, A_2 . These hypermultiplets correspond to the light BPS dyons, monopoles and quarks which are specified through the appropriate quantum numbers $(n_e, n_m)_n$. Here n_e and n_m are the electric and magnetic charges of $U(1)_c$, respectively, whereas n is the $U(1)$ charge. The mass of the BPS state is specified by

$$M_{\text{BPS}} = |n_e a_2 + n_m a_{2D} + n a_1|, \quad (3.6)$$

where a_{2D} is a scalar component of the chiral superfield A_{2D} . This \mathcal{L}_{HM} part should be added to the effective Lagrangian as new degrees of freedom if we focus on the singular points in the moduli space.

The soft term $\mathcal{L}_{\text{soft}}$ is given by

$$\mathcal{L}_{\text{soft}} = \int d^2\theta \left[\mu_2 U(A_1, A_2) + \frac{1}{2} \mu_1 A_1^2 + \lambda A_1 \right] + h.c., \quad (3.7)$$

provided that the condition $\mu_i^2, \lambda \ll \Lambda^2$ is satisfied. Here $U(A_2, A_1)$ is a low energy effective superfield given by

$$U(A_2, A_1) = u(a_2, a_1) + \theta^2 F_2 \left. \frac{\partial u}{\partial a_2} \right|_{a_1} + \theta^2 F_1 \left. \frac{\partial u}{\partial a_1} \right|_{a_2}, \quad (3.8)$$

where u represents a modulus field whose form in a weak coupling limit is $u = \text{Tr}(A_2^2)$, and F_1 and F_2 are the auxiliary fields of A_1 and A_2 , respectively.

In order to obtain an exact description of the effective Lagrangian, we need to find the explicit form of the prepotential \mathcal{F} and the effective coupling b_{ij} . To derive these, let us consider the monodromy transformations around the singular points of the moduli space. Suppose that the moduli space is parameterized by the vector multiplet scalars a_2, a_1 and their duals a_{2D}, a_{1D} which are defined as $a_{iD} = \partial \mathcal{F} / \partial a_i$ ($i = 1, 2$). These variables are transformed into their linear combinations by the monodromy transformation. In our case, the monodromy transformations form a subgroup of $Sp(4, \mathbf{R})$, which leaves the effective Lagrangian $\mathcal{L}_{\text{VM}} + \mathcal{L}_{\text{HM}}$ invariant, and the general formula is found to be [17]

$$\begin{pmatrix} a_{2D} \\ a_2 \\ a_{1D} \\ a_1 \end{pmatrix} \rightarrow \begin{pmatrix} \alpha a_{2D} + \beta a_2 + p a_1 \\ \gamma a_{2D} + \delta a_2 + q a_1 \\ a_{1D} + p(\gamma a_{2D} + \delta a_2) - q(\alpha a_{2D} + \beta a_2) - p q a_1 \\ a_1 \end{pmatrix}, \quad (3.9)$$

where $\begin{pmatrix} \alpha & \beta \\ \gamma & \delta \end{pmatrix} \in SL(2, \mathbf{Z})$ and $p, q \in \mathbf{Q}$. Note that this monodromy transformation for the combination (a_{2D}, a_2, a_1) is exactly the same as that for $\mathcal{N} = 2$ $SU(2)$ SUSY QCD with $N_f = 2$ massive quark hypermultiplets, if we regard a_1 as the common mass m of the hypermultiplets such that $m = \sqrt{2}a_1$. This fact means that the $U(1)$ gauge interaction part only plays the role of the mass term for the $SU(2)$ gauge dynamics. This observation is consistent with our assumptions. On the other hand, the $SU(2)$ dynamics plays an important role for the $U(1)$ gauge interaction through the hypermultiplet part, as can be seen from the transformation law of a_{1D} . This monodromy transformation is also used to derive dual variables associated with the BPS states. As a result, the prepotential of our theory turns out to be essentially the same as the result in Ref. [9] with the additional relation $m = \sqrt{2}A_1$,

$$\mathcal{F}(A_2, A_1, \Lambda, \Lambda_L) = \mathcal{F}_{SU(2)}^{(SW)}(A_2, m, \Lambda) \Big|_{m=\sqrt{2}A_1} + CA_1^2, \quad (3.10)$$

where the first term on the right hand side is the prepotential of $\mathcal{N} = 2$ SUSY QCD with hypermultiplets having the same mass m , and C is a free parameter. The freedom of the parameter C is used to determine the scale of the Landau pole relative to the scale of the $SU(2)$ dynamics. For instance, taking $C = 4\pi i$ leads to the value of the Landau pole $\Lambda_L \sim 10^{17-18}$ (for more detail, see Appendix A and also [11, 10]).

Now that we have obtained the explicit form of the effective Lagrangian, let us move on to the analysis of the potential.

3.2 Effective potential

We can write down the effective potential from (3.1) with (3.3), (3.5) and (3.7). After using the equation of motion for the auxiliary fields D_i, F_i, F_M and $F_{\tilde{M}}$ ($i = 1, 2$) of the superfields V_i, A_i, M and \tilde{M} , the effective potential is written as [¶]

$$V = b_{ij}F_iF_j^\dagger + \frac{1}{2}b_{ij}D_iD_j + |F_M|^2 + |F_{\tilde{M}}|^2. \quad (3.11)$$

Here

$$D_1 = \frac{b_{12} - nb_{22}}{\det b}(|M^r|^2 - |\tilde{M}_r|^2), \quad (3.12)$$

$$D_2 = \frac{-(b_{11} - nb_{12})}{\det b}(|M^r|^2 - |\tilde{M}_r|^2), \quad (3.13)$$

$$F_1 = \frac{-1}{\det b} \left[\sqrt{2}M_r^\dagger \tilde{M}^{r\dagger} (nb_{22} - b_{12}) + X^\dagger \right], \quad (3.14)$$

$$F_2 = \frac{1}{\det b} \left[\sqrt{2}M_r^\dagger \tilde{M}^{r\dagger} (nb_{12} - b_{11}) + Y^\dagger \right], \quad (3.15)$$

$$F_M = -\sqrt{2}(a_2^\dagger + na_1^\dagger)\tilde{M}^{r\dagger}, \quad (3.16)$$

$$F_{\tilde{M}} = -\sqrt{2}(a_2^\dagger + na_1^\dagger)M_r^\dagger, \quad (3.17)$$

[¶] We assume that the potential is described by the proper variables associated with the light BPS states. For example, the variable a_2 is understood implicitly as $-a_{2D}$ when we consider the effective potential for the monopole.

where $\det b = b_{11}b_{22} - b_{12}^2$ and

$$|M^r|^2 = M^r M_r^\dagger, \quad |\tilde{M}_r|^2 = \tilde{M}_r \tilde{M}^{r\dagger}, \quad (3.18)$$

$$X = b_{22}(\lambda + \mu_1 a_1) + \mu_2 \left(b_{22} \frac{\partial u}{\partial a_1} - b_{12} \frac{\partial u}{\partial a_2} \right), \quad (3.19)$$

$$Y = b_{12}(\lambda + \mu_1 a_1) + \mu_2 \left(-b_{11} \frac{\partial u}{\partial a_2} + b_{12} \frac{\partial u}{\partial a_1} \right). \quad (3.20)$$

After plugging the solution (3.12)-(3.17) into (3.11), the potential is rewritten in terms of a_1, a_2, M, \tilde{M} . The result is

$$\begin{aligned} V(a_2, a_1, M, \tilde{M}) = & S \left[(|M^r|^2 - |\tilde{M}_r|^2)^2 + 4|M^r \tilde{M}_r|^2 \right] + 2T(|M^r|^2 + |\tilde{M}_r|^2) + U \\ & + \frac{\sqrt{2}}{\det b} \left[M_r^\dagger \tilde{M}^{r\dagger} (nX - Y) + h.c. \right]. \end{aligned} \quad (3.21)$$

Here we have defined

$$S \equiv \frac{1}{2b_{22}} + \frac{(b_{12} - nb_{22})^2}{2b_{22} \det b}, \quad (3.22)$$

$$T \equiv |a_2 + na_1|^2, \quad (3.23)$$

$$\begin{aligned} U \equiv & \frac{1}{\det b} \left[b_{22} \left| (\lambda + \mu_1 a_1) + \mu_2 \frac{\partial u}{\partial a_1} \right|^2 + b_{11} \mu_2^2 \left| \frac{\partial u}{\partial a_2} \right|^2 \right. \\ & \left. - \left\{ (\lambda + \mu_1 a_1) \mu_2 b_{12} \frac{\partial u^\dagger}{\partial a_2^\dagger} + \mu_2^2 b_{12} \frac{\partial u^\dagger}{\partial a_1^\dagger} \frac{\partial u}{\partial a_2} + h.c. \right\} \right]. \end{aligned} \quad (3.24)$$

Let us consider the stationary conditions in the hypermultiplet directions M and \tilde{M} ,

$$0 = \frac{\partial V}{\partial M^\dagger} = S \left[2(|M|^2 - |\tilde{M}|^2)M + 4(M\tilde{M})\tilde{M}^\dagger \right] + 2TM + \frac{\sqrt{2}}{\det b} \tilde{M}^\dagger (nX - Y), \quad (3.25)$$

$$0 = \frac{\partial V}{\partial \tilde{M}^\dagger} = S \left[2(|M|^2 - |\tilde{M}|^2)(-\tilde{M}) + 4(M\tilde{M})M^\dagger \right] + 2T\tilde{M} + \frac{\sqrt{2}}{\det b} M^\dagger (nX - Y), \quad (3.26)$$

where we have suppressed the indices for simplicity. From these equations, we find

$$2 \left[S(|M|^2 + |\tilde{M}|^2) + T \right] (|M|^2 - |\tilde{M}|^2) = 0. \quad (3.27)$$

Since $S > 0$ and $T > 0$, we obtain the condition $|M| = |\tilde{M}|$. This allows us to re-express M and \tilde{M} as

$$\begin{aligned} |M| &= |\tilde{M}| \equiv \mathcal{M}, \\ M &\equiv \mathcal{M} e^{i\vartheta}, \quad \tilde{M} \equiv \mathcal{M} e^{i\tilde{\vartheta}}. \end{aligned} \quad (3.28)$$

Using the condition $|M| = |\tilde{M}|$, we find

$$0 = \frac{\partial V}{\partial M^\dagger} = 4S\mathcal{M}^3 e^{i\vartheta} + 2T\mathcal{M} e^{i\vartheta} + \frac{\sqrt{2}}{\det b} \mathcal{M} e^{-i\tilde{\vartheta}} (nX - Y), \quad (3.29)$$

$$0 = \frac{\partial V}{\partial \tilde{M}^\dagger} = 4S\mathcal{M}^3 e^{-i\tilde{\vartheta}} + 2T\mathcal{M} e^{-i\tilde{\vartheta}} + \frac{\sqrt{2}}{\det b} \mathcal{M} e^{i\vartheta} (nX - Y)^\dagger. \quad (3.30)$$

These equations fix the phases ϑ and $\tilde{\vartheta}$ as

$$e^{i(\vartheta+\tilde{\vartheta})} = \pm \left[\frac{nX - Y}{(nX - Y)^\dagger} \right]^{\frac{1}{2}}. \quad (3.31)$$

Substituting this solution into (3.30) gives

$$\mathcal{M} \left[4S\mathcal{M}^2 + 2T \pm \frac{\sqrt{2}}{\det b} |nX - Y| \right] = 0. \quad (3.32)$$

We find the following solution for the above equation

$$1) \mathcal{M} = 0, \quad (3.33)$$

$$2) \mathcal{M}^2 = -\frac{T}{2S} \mp \frac{\sqrt{2}}{4S \det b} |nX - Y|. \quad (3.34)$$

The positivity of \mathcal{M}^2 requires us to take the plus sign in (3.34). Corresponding to the solutions (3.33) and (3.34), we have the following forms of the scalar potentials

$$1) V(a_2(u, a_1), a_1) = U, \quad (3.35)$$

$$2) V(a_2(u, a_1), a_1) = U - 4S\mathcal{M}^4. \quad (3.36)$$

The solution (3.36) where the light hypermultiplet acquires a vacuum expectation value is energetically favored because $S > 0$. The potential minimum is expected to emerge at the singular points on the moduli space since the hypermultiplets appear in the theory as the light BPS states there. In addition, the solutions are stable in the \mathcal{M} direction. This is because they are unique solutions and have a lower energy than (3.33). Furthermore the potential is dominated by \mathcal{M}^4 term with a positive coefficient for a large value of \mathcal{M} . On the other hand, the solution (3.35) describes the behaviour away from the singular points. It smoothly connects with the solution (3.36).

In the next section we examine the effective potential (3.36) numerically. The potential is a function of the periods a_{2D}, a_2 and the effective couplings τ_{ij} . In order to perform the analysis of the potential, we need their explicit forms. Their detailed derivation was given in [11, 10]. In the Appendix A, we assemble these forms and also display other necessary formulas for the analysis of the potential.

4 Numerical analysis

4.1 Singular points

As explained in the previous section, the minimum is expected to appear at the singular point since it is energetically favored due to the non-zero condensation of the light BPS state (see eq. (3.36)). Thus, let us first investigate the singular points before analyzing the effective potential at the singular point.

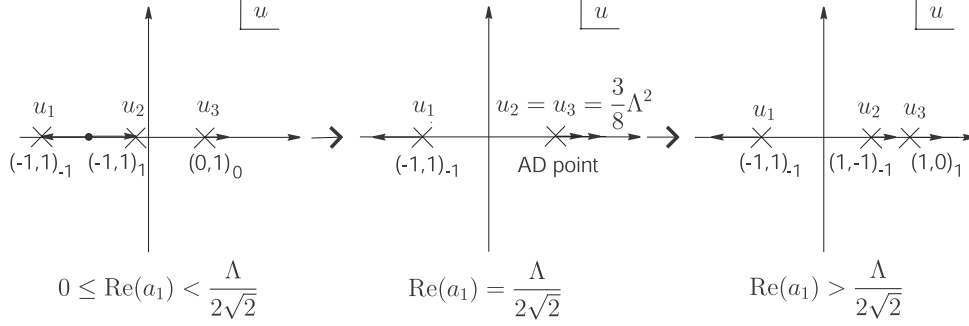


Figure 1: Flow of the singular points as $\text{Re}(a_1)$ increases with $\text{Im}(a_1) = 0$.

The singular points on the moduli space are determined by the cubic polynomial [9]. The solutions of the cubic polynomial give the positions of the singular points in the u -plane. In the case $N_c = N_f = 2$ with a common hypermultiplet mass m , which is regarded as the modulus $\sqrt{2}a_1$ here, the solution is easily obtained as

$$u_1 = -m\Lambda - \frac{\Lambda^2}{8} \Big|_{m=\sqrt{2}a_1}, \quad u_2 = m\Lambda - \frac{\Lambda^2}{8} \Big|_{m=\sqrt{2}a_1}, \quad u_3 = m^2 + \frac{\Lambda^2}{8} \Big|_{m=\sqrt{2}a_1}. \quad (4.1)$$

Let us first consider the case $\text{Im}(a_1) = 0$. The flow of the singular points with respect to a_1 is sketched in Fig. 1. For $a_1 = 0$, the singular points appear at $u_1 = u_2 = -\Lambda^2/8$ and $u_3 = \Lambda^2/8$, which correspond to the dyon and the monopole BPS states with quantum numbers $(n_e, n_m)_n = (-1, 1)_0$ and $(0, 1)_0$, respectively. When switching on a_1 , the degenerate dyon point splits into two singular points u_1 and u_2 , whose BPS states are dyons with quantum numbers $(-1, 1)_{-1}$ (left dyon) and $(-1, 1)_1$ (right dyon), respectively. As a_1 is increasing, these singular points, u_1 and u_2 , are moving to the left and the right on the real u -axis. The two singular points, u_2 and u_3 , collide and coincide at the so-called Argyres-Douglas (AD) point [18] ($u = \frac{3\Lambda^2}{8}$) for $a_1 = \Lambda/(2\sqrt{2})$, where it is believed that the theory becomes superconformal. As a_1 increases further, there appear two singular points u_2 and u_3 again, and the quantum numbers of the corresponding BPS states, $(-1, 1)_1$ at u_2 and $(0, 1)_0$ at u_3 , change into $(1, 1)_{-1}$ (right dyon) and $(1, 0)_1$ (quark), respectively. The singular point u_3 is then moving away to the right faster than u_2 . Note that for $\text{Im}(a_1) = 0$, it is not necessary to consider the case for $a_1 < 0$, since the result for $a_1 < 0$ can be obtained by exchanging $u_1 \leftrightarrow u_2$, as can be seen from the first two equations in eq. (4.1).

4.2 Numerical calculation

Let us examine the effective potential (3.36) numerically. Since the potential minimum appears at the singular point, it is sufficient to investigate the behavior of the effective potential around the singular point. This consideration simplifies the numerical calculations. The singular point is specified by (4.1) and thus the potential at the singular point becomes just a function of a_1 . In the following we investigate the effective potential at some fixed values of a_1 and see how the

minimum appears at the singular point. Then we examine the evolution of the minimum by varying a_1 . In the whole numerical analysis, we take $\Lambda = 2\sqrt{2}$. The values of μ_i and λ will be taken so that the conditions $\mu_i \ll \Lambda$ and $\lambda \ll \Lambda^2$ are satisfied.

Since the singular points in the moduli space exhibit different behaviors according to the value of a_1 , let us separate the a_1 region into three parts, namely, (i) $0 \leq \text{Re}(a_1) < \frac{\Lambda}{2\sqrt{2}}$, (ii) $\text{Re}(a_1) = \frac{\Lambda}{2\sqrt{2}}$, (iii) $\text{Re}(a_1) > \frac{\Lambda}{2\sqrt{2}}$. In each region, we also consider the $\text{Im}(a_1)$ direction. Let us first analyze the case $\mu_1 = \lambda = 0$. In this case, the soft term $\mathcal{L}_{\text{soft}}$ is simply

$$\mathcal{L}_{\text{soft}} = \mu_2^2 \int d^2\theta U(A_2, A_1) + h.c.. \quad (4.2)$$

Note that now there exists symmetry between two BPS states at the singular points u_1 and u_2 for the region (i). They are invariant under the interchanges $a_1 \leftrightarrow -a_1$ and $n \leftrightarrow -n$ (see (3.6) and (4.1)).

(i) $0 \leq \text{Re}(a_1) < \frac{\Lambda}{2\sqrt{2}}$

In this region, there are two dyons corresponding to u_1 (left dyon) and u_2 (right dyon) and a monopole corresponding to u_3 . As anticipated in the discussion in section 3, there are three potential minima at these singular points. The left figure in Fig. 2 shows the effective potential around the monopole singular point along the real u -axis for several fixed values of a_1 with $\mu_2 = 0.1$. There potential has a minimum at the singular point. The upper solid curve shows

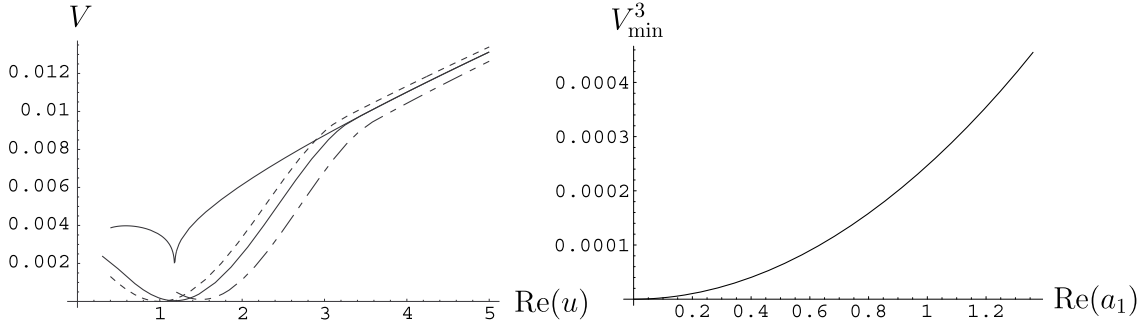


Figure 2: The left figure shows the plots of the potential around the monopole singular point as a function of real u with $a_1 = 0.2$ (dotted), 0.3 (solid) and 0.4 (dash-dotted). For the case $a_1 = 0.3$, the potential is shown both with (bottom curve) and without (upper curve) condensation. The right figure shows the evolution of the potential minimum at the monopole singular point V_{\min}^3 as a function of real a_1 .

the potential without the monopole condensation (3.35) and the bottom solid curve includes the condensation (3.36) for $a_1 = 0.3$. The cusps in the potential are smoothed out by introducing BPS states. It shows that the BPS state enjoys correct degrees of freedom. The other curves are plots for $a_1 = 0.2$ (dotted) and $a_1 = 0.4$ (dash-dotted). Note that the energy of the potential minimum is not zero except $a_1 = 0$ as we will show below. Now we examine how this minimum evolves as a_1 varies. The right figure in Fig. 2 shows the evolution of the potential minimum

at the monopole singular points V_{\min}^3 as a function of a_1 with $\mu_2 = 0.1$ and $\text{Im}(a_1) = 0$. As a_1 is decreasing, V_{\min}^3 monotonically decreases and $V_{\min}^3 = 0$ at $a_1 = 0$. The behavior of V_{\min}^3 for

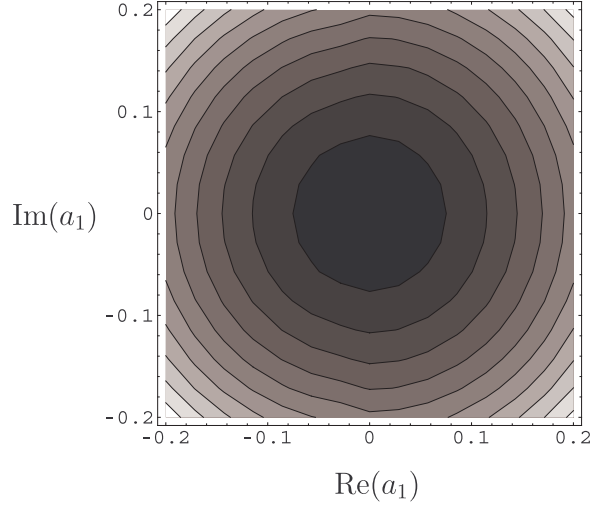


Figure 3: The contour plot at monopole singular point as a function of complex a_1 .

complex values of a_1 is shown as the contour plot in Fig. 3. The dark (light) color shows lower (higher) value of the effective potential. Thus, the potential minimum V_{\min}^3 is a SUSY vacuum at $\text{Re}(a_1) = \text{Im}(a_1) = 0$.

A similar analysis can be performed for the other singular points. The evolution of the potential energy at the right dyon singular point V_{\min}^2 as a function of $\text{Re}(a_1)$ with $\mu_2 = 0.1$ and $\text{Im}(a_1) = 0$ is shown in Fig. 4. The evolution of the effective potential at the left dyon singular point V_{\min}^1 has the same behavior as V_{\min}^2 since the singular points at u_1 and u_2 get interchanged under $a_1 \leftrightarrow -a_1$ and $n \leftrightarrow -n$ as mentioned in the previous subsection.

We have seen that the theory has two SUSY vacua at the monopole and (degenerate) dyon singular points at $a_1 = 0$. This result can be understood from the fact that the moduli structure

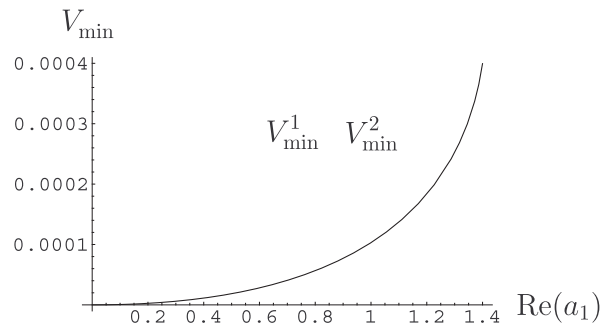


Figure 4: Plots for the evolution of the minima at the left and the right dyon singular points.

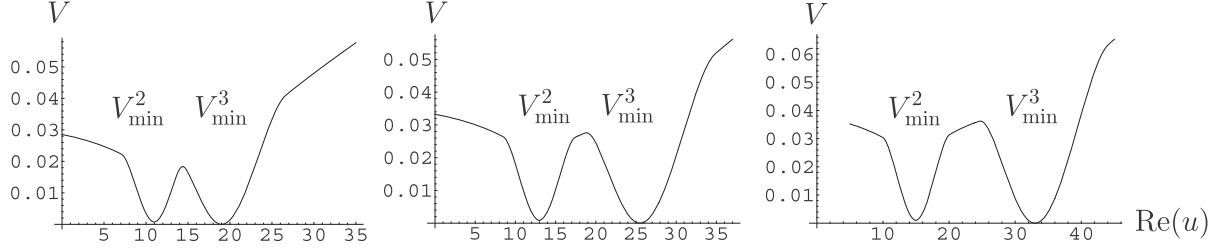


Figure 5: Plots of the potential along real u -axis with the values $a_1 = 4, 4.5, 5$ from left to right.

of $\mathcal{L}_{\text{SUSY}}$ for vanishing a_1 is the same as the one of $\mathcal{N} = 2$ $SU(2)$ theory with $N_f = 2$ massless flavors. Recall that $\mathcal{L}_{\text{SUSY}}$ includes the prepotential $\mathcal{F}_{SU(2)}^{(SW)}$ in (3.10) which describes the moduli space u . For vanishing mass ($a_1 = 0$), this prepotential is the same as that of $\mathcal{N} = 2$ $SU(2)$ with $N_f = 2$ massless flavors which has a \mathbf{Z}_2 symmetry, $u \leftrightarrow -u$ [9]. The soft SUSY breaking term $\mathcal{L}_{\text{soft}}$ with $\mu_1 = \lambda = 0$ has the effect of lifting up the potential in all of moduli space except at the monopole and the dyon singular points for $a_1 = 0$. The remaining vacua exhibit the \mathbf{Z}_2 symmetry.

Below we shall show that when μ_1 and λ are switched on, SUSY at these dyon and monopole points is broken dynamically.

(ii) $\text{Re}(a_1) = \frac{\Lambda}{2\sqrt{2}}$

At the point $a_1 = \frac{\Lambda}{2\sqrt{2}}$ (AD point), the two potential minima at the right dyon singular point V_{\min}^2 and at the monopole singular point V_{\min}^3 coincide. As we have mentioned, it is expected that the theory becomes superconformal. However, we have no knowledge of the correct description of the theory at this point.

(iii) $\text{Re}(a_1) > \frac{\Lambda}{2\sqrt{2}}$

In this region, there are again three singular points and correspondingly three potential minima, V_{\min}^1 at u_1 (left dyon), V_{\min}^2 at u_2 (right dyon) and V_{\min}^3 at u_3 (quark). Fig. 5 shows the effective potential along the real u axis around the right dyon and the quark singular points for several values of a_1 . We note that the energy at the potential minimum is not zero except certain point. The evolutions of the two minima at the right dyon and the quark singular points V_{\min}^2 and V_{\min}^3 are depicted in Fig. 6. The potential energies V_{\min}^2 and V_{\min}^3 approach zero as a_1 is decreasing, while the evolution of the potential energy at the singular point u_1 is the same as for $0 \leq \text{Re}(a_1) < \Lambda/(2\sqrt{2})$. Thus, there are runaway directions along the flow of the right dyon and the quark singular points. We can find the same global structure along the flows of these two singular points for general complex a_1 values.

The evolutions of the potential energies according the flows of the singular points along the real u -axis are simultaneously plotted in Fig. 7. The theory has SUSY vacua at $a_1 = 0$ and infinity, and no (local) SUSY breaking vacuum. However, this analysis gives us an important

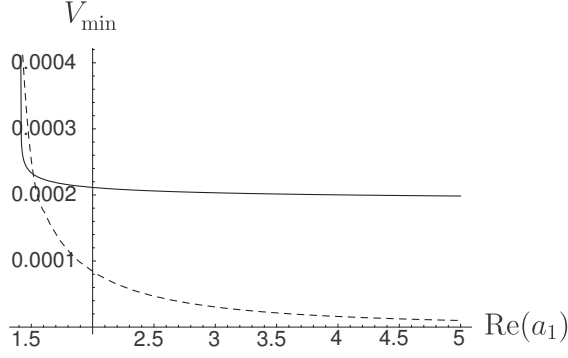


Figure 6: The evolutions of the potential energies V_{\min}^2 (solid) and V_{\min}^3 (dashed).

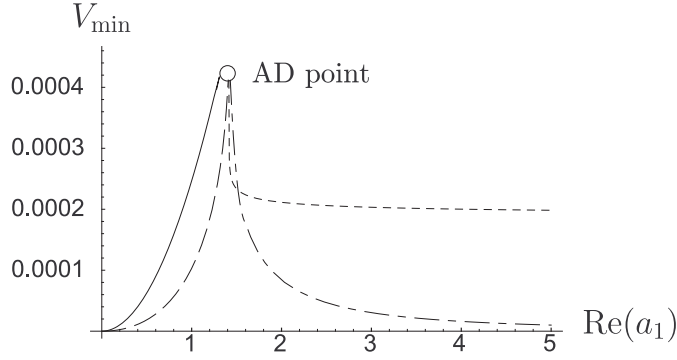


Figure 7: Global structure of vacuum. Solid and dashed curves show the evolutions of the potential energies at the monopole and left(right) dyon points for $0 \leq \text{Re}(a_1) < \Lambda/(2\sqrt{2})$. The potential energies at the right dyon(dotted) and quark(dash-dotted) points for $\text{Re}(a_1) > \Lambda/(2\sqrt{2})$ are also plotted.

piece of information. In the presence of the soft term (4.2), the gauge dynamics favors the monopole and the dyon points at $a_1 = 0$ as SUSY vacua besides the runaway vacua. It implies that if we can add certain terms to (4.2) which produce a vacuum at a point different from $a_1 = 0$ at the classical level, SUSY is dynamically broken as a consequence of the discrepancy of SUSY conditions between the classical and the quantum theories. Actually, turning on the mass μ_1 and the FI parameter λ realizes such a situation. In this case, the classical vacuum is at $a_1 = -\lambda/\mu_1$, different from the point $a_1 = 0$ which the dynamics favors. A resultant SUSY breaking vacuum is realized at non-zero value of a_1 . This is very similar to the SUSY breaking mechanism discussed in the Izawa-Yanagida-Intriligator-Thomas model in $\mathcal{N} = 1$ SUSY gauge theory [5, 6]. We show a schematic picture of our situation in Fig. 8.

Let us see in detail how this works for non-zero values of μ_1, μ_2 and λ . First we investigate the case $0 \leq \text{Re}(a_1) < \Lambda/(2\sqrt{2})$. Fig. 9 shows the evolution of the potential energies at the monopole point V_{\min}^3 for several values of λ as a function of $\text{Re}(a_1)$ with $\mu_1 = \mu_2 = 0.1$.

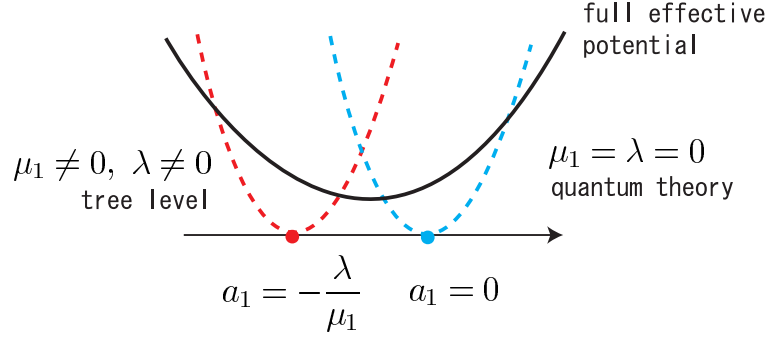


Figure 8: Schematic picture of SUSY breaking mechanism

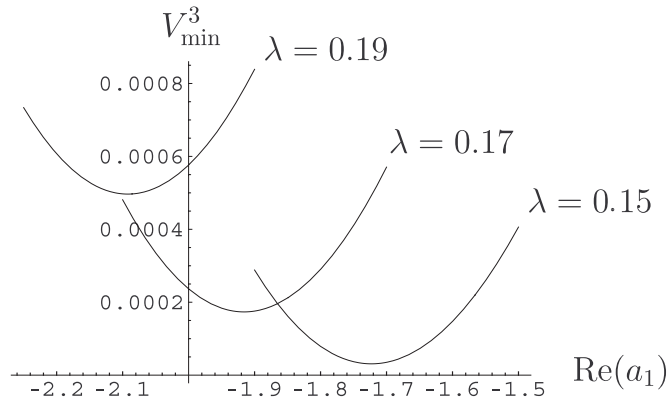


Figure 9: Local SUSY breaking minimum at the monopole singular point for $\mu_1 = \mu_2 = 0.1$ and $\lambda = 0.15, 0.17, 0.19$ from bottom to top.

The potential minimum is no longer realized at $a_1 = 0$, but the location is shifted to negative values of $\text{Re}(a_1)$ as is expected from the discussion in the previous paragraph (see also Fig. 8). Furthermore, the potential energy has a non-zero value and therefore SUSY is dynamically broken. The potential energy becomes large as λ is increasing. This is expected from the fact that the effective potential behaves as $V \sim \lambda^2$ (see (3.24) and (3.36)). We also find that the potential minimum at the monopole point is stable for general complex values of a_1 (for the $\mu_1 = \lambda = 0$ case, see Fig. 3).

The same situation occurs at the degenerate dyon singular point. Recall that for vanishing μ_1 and λ the theory has vacua at the degenerate dyon point $(u, a_1) = (-\Lambda^2, 0)$ and at the monopole point $(u, a_1) = (\Lambda^2, 0)$. These two vacua are transformed into each other under the \mathbf{Z}_2 symmetry $u \leftrightarrow -u$. Since turning on μ_1 and λ does not break this symmetry, it is also expected that SUSY is dynamically broken at the degenerate dyon point as it is shifted towards the negative direction of $\text{Re}(a_1)$. Therefore we now have two SUSY breaking minima at the degenerate dyon point and at the monopole point.

In order to see the global structure of the effective potential we also need to investigate

the potential for $\text{Re}(a_1) > \Lambda/(2\sqrt{2})$. Fig. 10 shows the potential energy around the quark singular point V_{\min}^3 as a function of $\text{Re}(u)$ and the evolution of V_{\min}^3 as a function of $\text{Re}(a_1)$ with $\mu_1 = \mu_2 = 0.1$ and $\lambda = 0.15$. Notably, the potential energy becomes large as a_1 is increasing. This behavior is completely different from the one of the $\mu_1 = \lambda = 0$ case. This difference can be understood from the classical potential (2.4). Since we are considering the Coulomb branch, substitute (2.5) with $q = \tilde{q} = 0$ into (2.4). Then we obtain

$$V = 2\mu_2^2 g^2 a_2^2 + e^2 |\lambda + \mu_2 a_1|^2. \quad (4.3)$$

For large values of a_1 the term $e^2 \mu_2^2 |a_1|^2$ is dominant. Therefore the potential energy increases monotonically with growing a_1 . We find that the potential energies at the left and right dyon singular points also have the same structure.

A qualitative picture of the evolutions of the potential minima is depicted in Fig. 11.

Now we have seen that there are two SUSY breaking minima and that there is no longer any runaway direction on the Coulomb branch. It appears that the two SUSY breaking minima are global ones, but there is still a possible SUSY vacuum on the Higgs branch whose existence in the classical theory is shown in (2.7). It is known that there are no quantum corrections on the Higgs branch [19]. Thus, at the quantum level, the SUSY vacuum on the Higgs branch is still left. In the next section, we discuss the decay rate from the local SUSY breaking vacua at the monopole and dyon singular points to the SUSY vacuum on the Higgs branch and show that the local vacua can actually be meta-stable with an appropriate choice of parameters.

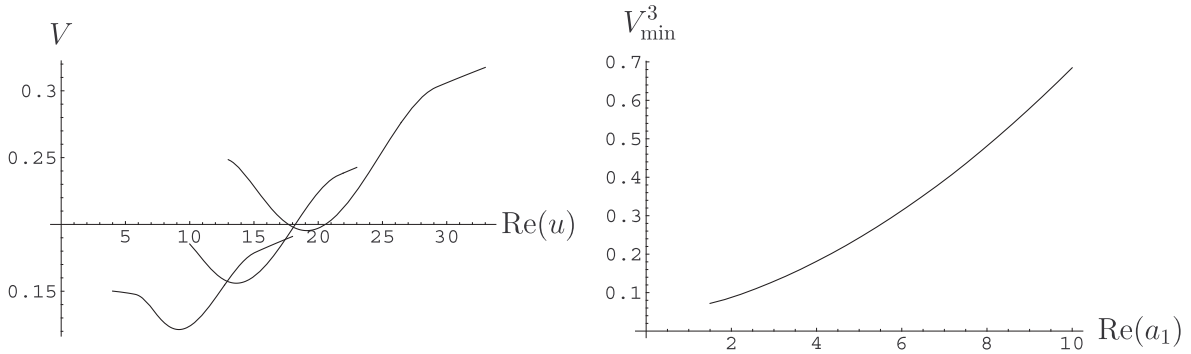


Figure 10: The left figure shows the effective potential around the quark singular point with $a_1 = 2, 2.5, 3$ from the bottom to the top. The right figure shows the evolution of the potential minimum at the quark singular point as a function of real a_1 with $\mu_1 = \mu_2 = 0.1$ and $\lambda = 0.15$.

5 Decay rate of the local vacuum

In this section, we estimate the decay rate from the SUSY breaking local minima on the Coulomb branch to the SUSY vacuum on the Higgs branch.

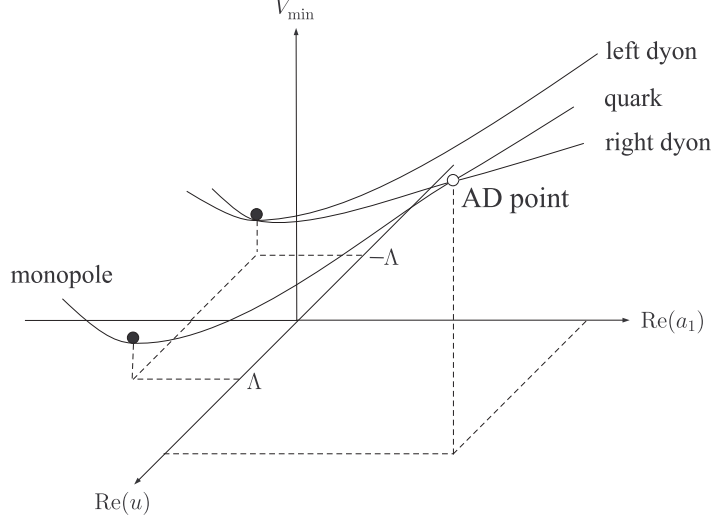


Figure 11: Qualitative picture of the evolutions of the potential minima.

The local minimum at the monopole point on the Coulomb branch is approximately given by the point $C : (a_1, a_2) \sim (-\lambda/\mu_1, \Lambda)$, $q = \tilde{q} = 0$ while the Higgs SUSY vacuum is at H , (2.7) (see Fig. 12). The distance between the vacua at Coulomb and Higgs branches, $|\overrightarrow{CH}|$, is given by

$$|\overrightarrow{CH}|^2 = 4(|u|^2 + |v|^2) + \left(\frac{\lambda}{\mu_1}\right)^2 + \Lambda^2 \equiv L^2. \quad (5.4)$$

We parameterize a point between C and H by the vector

$$\begin{aligned} \vec{p}(s) &\equiv (a_1, a_2, q_{r=1}, q_{r=2}, \tilde{q}_{r=1}, \tilde{q}_{r=2}) \\ &= s \left(\frac{\lambda}{\mu_1}, -\Lambda, \begin{pmatrix} u \\ v \end{pmatrix}, \begin{pmatrix} v \\ -u \end{pmatrix}, \begin{pmatrix} u \\ v \end{pmatrix}, \begin{pmatrix} v \\ -u \end{pmatrix} \right) + \left(-\frac{\lambda}{\mu_1}, \Lambda, \mathbf{0} \right), \end{aligned} \quad (5.5)$$

where $0 \leq s \leq 1$. The parameter value $s = 0$ corresponds to the Coulomb vacuum while $s = 1$ corresponds to the Higgs vacuum. Substituting (5.5) into the classical potential (2.4), we have

$$V(s) = V(\vec{p}(s)) \equiv (1-s)^2(s^2\beta_1 + \beta_2), \quad (5.6)$$

where

$$\beta_1 = 8 \left(\Lambda - \frac{\lambda}{\mu_1} \right)^2 (|u|^2 + |v|^2) + e^2 \lambda^2, \quad \beta_2 = 2\mu_2^2 g^2 \Lambda^2. \quad (5.7)$$

Now we show that there is a reasonable parameter region in which the local vacuum at the Coulomb branch, C , is meta-stable. We take the following parameter region, $\Lambda \gg \lambda/\mu_1$ and $\lambda/\mu_2^2 \gg g^2$, so that

$$\frac{\beta_1}{\beta_2} \sim \frac{\lambda}{\mu_2^2 g^2} \gg 1, \quad (5.8)$$

6 Conclusion and discussion

We investigated an $\mathcal{N} = 2$, $SU(2) \times U(1)$ supersymmetric gauge theory with $N_f = 2$ massless flavors perturbed by soft terms (2.3): mass terms for A_1 and A_2 and a term linear in A_1 , a Fayet-Iliopoulos term. The soft terms break the $\mathcal{N} = 2$ SUSY down to $\mathcal{N} = 1$.

We argued that when the parameters in the soft terms are small compared to the dynamical scale we can perform a reliable non-perturbative analysis based on the Seiberg-Witten solution. Our analysis revealed an interesting setup: On the Coulomb branch SUSY is dynamically broken in a manner reminiscent of the Izawa-Yanagida-Intriligator-Thomas model. A local minimum emerges, but no runaway SUSY vacua survive. On the Higgs branch, however, the SUSY vacua present at tree level should survive quantum corrections. The local minimum on the Coulomb branch decays into the Higgs branch vacuum, but not surprisingly, the values of the parameters can be chosen such that it is very long-lived, *i.e.* meta-stable.

We chose a model simple enough to be able to perform a thorough analysis. As such, it is too poor to serve as a basis for any realistic phenomenology. However, we think that it once again shows the richness of supersymmetric gauge theories in being able to provide instances of the most different kinds of properties, and in this respect we hope that our simple model, like our previous attempt [10], could provide clues for building realistic descriptions of a world with broken supersymmetry.

Acknowledgements

The work of N. O. is partly supported by the Grant-in-Aid for Scientific Research in Japan (#15740164). S. S. is supported by the bilateral program of Japan Society for the Promotion of Science and Academy of Finland, “Scientist Exchanges.”

Appendix

A Explicit form of the effective couplings

In this appendix, we show the explicit forms of the periods $a(u)$, $a_D(u)$, the effective couplings b_{ij} and other quantities such as $\frac{\partial u}{\partial a_i}$. They are necessary for the analysis of the potential (3.36) since the potential is a function of them. A more detailed derivation of these expressions can be found in [11, 10]. In the following, Λ is a $SU(2)$ dynamical scale and m is a common mass for the hypermultiplets, which is replaced with a_1 through the relation $m = \sqrt{2}a_1$ in the main body of the paper.

We first consider the periods a_{2D} and a_2 . Let us denote these as a_{21} and a_{22} respectively. These are given by

$$a_{2i} = -\frac{\sqrt{2}}{4\pi} \left(-\frac{4}{3}uI_1^{(i)} + 8I_2^{(i)} + \frac{m^2\Lambda^2}{8}I_3^{(i)} \left(-\frac{u}{12} - \frac{\Lambda^2}{32} \right) \right) - \frac{m}{\sqrt{2}}\delta_{i2}, \quad (\text{A.1})$$

with the elliptic integrals $I_s^{(1)}$ ($s = 1, 2, 3$) explicitly given by

$$I_1^{(1)} = \frac{iK(k')}{\sqrt{e_2 - e_1}}, \quad (\text{A.2})$$

$$I_2^{(1)} = \frac{ie_1}{\sqrt{e_2 - e_1}}K(k') + i\sqrt{e_2 - e_1}E(k'), \quad (\text{A.3})$$

$$I_3^{(1)} = \frac{-i}{(e_2 - e_1)^{3/2}} \left\{ \frac{1}{k + \tilde{c}}K(k') + \frac{4k}{1 + k} \frac{1}{\tilde{c}^2 - k^2} \Pi_1 \left(\nu, \frac{1 - k}{1 + k} \right) \right\}, \quad (\text{A.4})$$

where $k^2 = \frac{e_3 - e_1}{e_2 - e_1}$, $k'^2 = 1 - k^2 = \frac{e_2 - e_3}{e_2 - e_1}$, $\tilde{c} = \frac{c - e_1}{e_2 - e_1}$, and $\nu = -\left(\frac{k + \tilde{c}}{k - \tilde{c}}\right)^2 \left(\frac{1 - k}{1 + k}\right)^2$. Here e_i ($i = 1, 2, 3$) is a root of the elliptic curve for the $\mathcal{N} = 2$ $SU(2)$ QCD with massive $N_f = 2$ flavors

$$\begin{aligned} e_1 &= \frac{u}{24} - \frac{\Lambda^2}{64} - \frac{1}{8} \sqrt{u + \frac{\Lambda^2}{8} + \Lambda m} \sqrt{u + \frac{\Lambda^2}{8} - \Lambda m}, \\ e_2 &= \frac{u}{24} - \frac{\Lambda^2}{64} + \frac{1}{8} \sqrt{u + \frac{\Lambda^2}{8} + \Lambda m} \sqrt{u + \frac{\Lambda^2}{8} - \Lambda m}, \\ e_3 &= -\frac{u}{12} + \frac{\Lambda^2}{32}. \end{aligned} \quad (\text{A.5})$$

The formulae for $I_s^{(2)}$ are obtained from $I_s^{(1)}$ by exchanging the roots e_1 and e_2 . In eqs. (A.2)-(A.4), K , E and Π_1 are the complete elliptic integrals [22] given by

$$\begin{aligned} K(k) &= \int_0^1 \frac{dx}{[(1 - x^2)(1 - k^2 x^2)]^{1/2}}, \\ E(k) &= \int_0^1 dx \left(\frac{1 - k^2 x^2}{1 - x^2} \right)^{1/2}, \\ \Pi_1(\nu, k) &= \int_0^1 \frac{dx}{[(1 - x^2)(1 - k^2 x^2)]^{1/2} (1 + \nu x^2)}. \end{aligned} \quad (\text{A.6})$$

Next let us consider the effective coupling defined in eq. (3.4). The effective couplings τ_{22} and τ_{12} are obtained by

$$\tau_{22} = \frac{\partial a_{2D}}{\partial a_2} = \frac{\omega_1}{\omega_2}, \quad (\text{A.7})$$

$$\tau_{12} = \left. \frac{\partial a_{2D}}{\partial a_1} \right|_u - \tau_{22} \left. \frac{\partial a_2}{\partial a_1} \right|_u = -\frac{2z_0}{\omega_2}, \quad (\text{A.8})$$

where ω_i is the period of the Abelian differential,

$$\omega_i = 2I_1^{(i)} \quad (i = 1, 2), \quad (\text{A.9})$$

and z_0 is defined as

$$z_0 = -\frac{1}{\sqrt{e_2 - e_1}} F(\phi, k); \quad \sin^2 \phi = \frac{e_2 - e_1}{c - e_1}. \quad (\text{A.10})$$

Here $F(\phi, k)$ is the incomplete elliptic integral of the first kind given by

$$F(\phi, k) = \int_0^{\sin \phi} \frac{dt}{[(1-t^2)(1-k^2t^2)]^{1/2}}. \quad (\text{A.11})$$

The effective coupling τ_{11} is described in terms of the Weierstrass function

$$\tau_{11} = -\frac{1}{\pi i} \left[\log \sigma(2z_0) + \frac{4z_0^2}{\omega_2} I_2^{(1)} \right] + C. \quad (\text{A.12})$$

Here σ is the Weierstrass sigma function, and C is the constant in eq. (3.10).

We now define the Landau pole associated with the $U(1)$ interaction. In the ultraviolet region far away from the origin of the moduli space, the effective coupling is dominated by the $U(1)$ gauge interaction since the $SU(2)$ interaction is asymptotic free and small. As expected, the gauge coupling b_{11} is found to be a monotonically decreasing function of the large $|a_1|$ with fixed u , and vice versa. The Landau pole is defined as $|a_1| = \Lambda_L$ at which $b_{11} = 0$. The large Λ_L required in our assumption is realized by taking an appropriate value for C . In this paper, we fix $C = 4\pi i$, which corresponds to $\Lambda_L = 10^{17-18}$ in units of Λ [11, 10]. Fig. 13 shows the plot of the effective coupling b_{11} for $C = 4\pi i$ as a function of $\text{Re}(a_1)$ with $u = 4$. The cusps appear through the effect of the $SU(2)$ dynamics; their locations are specified by (4.1).

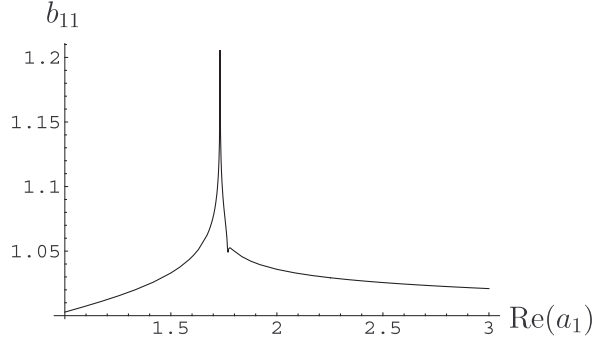


Figure 13: Plot of the effective coupling b_{11} as a function of $\text{Re}(a_1)$ with $u = 4$.

Finally we give the forms of $\frac{\partial u}{\partial a_1}$ and $\frac{\partial u}{\partial a_2}$. The former can be calculated as

$$\begin{aligned} \left. \frac{\partial u}{\partial a_1} \right|_{a_2} &= - \left. \frac{\partial u}{\partial a_1} \right|_{a_2} \left. \frac{\partial a_2}{\partial a_1} \right|_u = - \frac{1}{\omega_2} \left. \frac{\partial a_2}{\partial a_1} \right|_u \\ &= - \frac{1}{\pi} \left(\omega_2 \zeta(z_0) - 2z_0 \zeta\left(\frac{\omega_2}{2}\right) \right) = - \frac{m\Lambda^2}{16\pi} I_3^{(2)}. \end{aligned} \quad (\text{A.13})$$

The latter is simply given by

$$\left. \frac{\partial u}{\partial a_2} \right|_{a_1} = \frac{1}{\omega_2}. \quad (\text{A.14})$$

References

- [1] E. Witten, Phys. Lett. B **105** (1981) 267.
- [2] J. Wess and B. Zumino, Phys. Lett. B **49** (1974) 52; S. Ferrara, J. Iliopoulos and B. Zumino, Nucl. Phys. B **77** (1974) 413; M. T. Grisaru, W. Siegel and M. Rocek, Nucl. Phys. B **159** (1979) 429.
- [3] N. Seiberg, Phys. Lett. B **318** (1993) 469 [arXiv:hep-ph/9309335].
- [4] N. Seiberg, Phys. Rev. D **49** (1994) 6857 [arXiv:hep-th/9402044].
- [5] K. I. Izawa and T. Yanagida, Prog. Theor. Phys. **95** (1996) 829 [arXiv:hep-th/9602180].
- [6] K. A. Intriligator and S. D. Thomas, Nucl. Phys. B **473** (1996) 121 [arXiv:hep-th/9603158].
- [7] K. Intriligator, N. Seiberg and D. Shih, JHEP **0604** (2006) 021 [arXiv:hep-th/0602239].
- [8] N. Seiberg and E. Witten, Nucl. Phys. B **426** (1994) 19 [Erratum-ibid. B **430** (1994) 485] [arXiv:hep-th/9407087].
- [9] N. Seiberg and E. Witten, Nucl. Phys. B **431** (1994) 484 [arXiv:hep-th/9408099].
- [10] M. Arai, C. Montonen, N. Okada and S. Sasaki, Phys. Rev. D **76** (2007) 125009 [arXiv:0708.0668 [hep-th]].
- [11] M. Arai and N. Okada, Phys. Rev. D **64** (2001) 025024 [arXiv:hep-th/0103157]; Nucl. Phys. Proc. Suppl. **102** (2001) 219 [arXiv:hep-th/0103174].
- [12] H. Ooguri, Y. Ookouchi and C. S. Park, “Metastable vacua in perturbed Seiberg-Witten theories,” arXiv:0704.3613 [hep-th].
- [13] G. Pastras, “Non supersymmetric metastable vacua in $N = 2$ SYM softly broken to $N = 1$,” arXiv:0705.0505 [hep-th].
- [14] J. Marsano, H. Ooguri, Y. Ookouchi and C. S. Park, “Metastable Vacua in Perturbed Seiberg-Witten Theories, Part 2: Fayet-Iliopoulos Terms and Kähler Normal Coordinates,” arXiv:0712.3305 [hep-th].
- [15] L. Mazzucato, Y. Oz and S. Yankielowicz, JHEP **0711** (2007) 094 [arXiv:0709.2491 [hep-th]].
- [16] I. Bena, E. Gorbatov, S. Hellerman, N. Seiberg and D. Shih, JHEP **0611** (2006) 088 [arXiv:hep-th/0608157].
- [17] L. Alvarez-Gaume, M. Marino and F. Zamora, Int. J. Mod. Phys. A **13** (1998) 403 [arXiv:hep-th/9703072]; Int. J. Mod. Phys. A **13** (1998) 1847 [arXiv:hep-th/9707017].
- [18] P. C. Argyres and M. R. Douglas, Nucl. Phys. B **448** (1995) 93. [arXiv:hep-th/9505062].

- [19] P. C. Argyres, M. R. Plesser and N. Seiberg, Nucl. Phys. B **471** (1996) 159 [arXiv:hep-th/9603042].
- [20] S. R. Coleman, Phys. Rev. D **15** (1977) 2929 [Erratum-ibid. D **16** (1977) 1248].
- [21] M. J. Duncan and L. G. Jensen, Phys. Lett. B **291** (1992) 109.
- [22] A. Erdelyi et al., *Higher Transcendental Functions*, Vol. 1, McGraw-Hill, New York (1953).